Journal of Nanostructure in Chemistry (2020) 10:193–201
https://doi.org/10.1007/s40097-020-00341-1

ORIGINAL RESEARCH

Green synthesis of iron oxide nanoparticles by the aqueous extract of *Laurus nobilis* L. leaves and evaluation of the antimicrobial activity

Mina Jamzad[1] · **Maryam Kamari Bidkorpeh**[1]

Received: 9 December 2019 / Accepted: 9 May 2020 / Published online: 13 June 2020

Abstract

A valuable approach in green nanotechnology is the application of biomaterials in the synthesis of nanoparticles. In this project, we synthesized iron oxide nanoparticles in the phase of hematite (α-Fe_2O_3) by the aqueous extract of *Laurus nobilis* L. leaves in a simple and eco-friendly method. The nanoparticles were characterized using Ultraviolet–Visible spectroscopy (UV–Visible), Fourier transform infrared (FT-IR) spectroscopy, X-ray diffraction analysis (XRD), scanning electron microscopy (SEM), transfer electron microscopy (TEM) and energy-dispersive X-ray spectroscopy (EDS). The results showed that the nanoparticles are crystalline, almost spherical like and partly as a hexagonal shape with an average size of 8.03 ± 8.99 nm. The antimicrobial activity of the synthesized nanoparticles was evaluated against three bacteria and two fungi. The results showed that the nanoparticles are moderately effective on the Gram-positive bacterium of *Listeria monocytogenes* and the fungi *Aspergillus flavus* and *Penicillium spinulosum.* The nanoparticles synthesized by this green method could be potentially useful as antifungal and antibacterial compound and, may be considered as gas sensors, light photo-catalysis and, semiconductor.

Graphic abstract

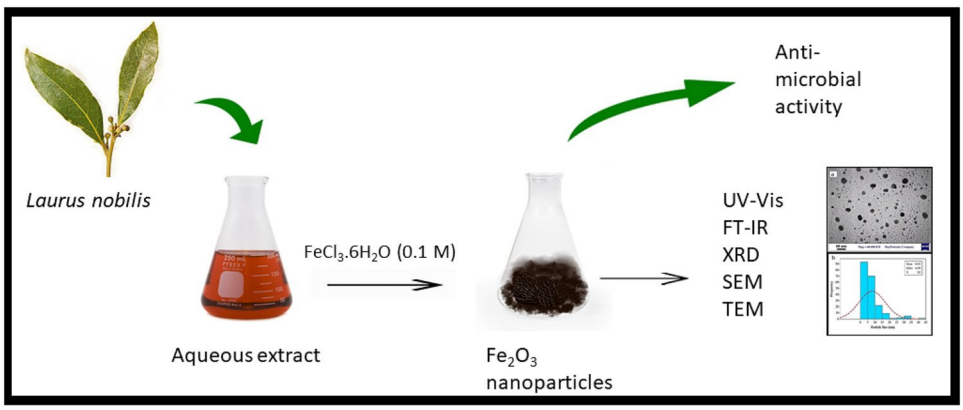

Keywords Hematite · XRD · *Laurus nobilis* extract · *Listeria monocytogenes* · *Aspregilus flavus*

Introduction

The goal of green chemistry is the development of chemical processes that reduce waste products and prevent environmental pollution. Nowadays the use of biomaterials as replacements for hazardous substances is a noteworthy approach in green nanotechnology [1]. Various organisms

✉ Mina Jamzad
m.jamzad@qodsiau.ac.ir; minajamzadiau@gmail.com

[1] Department of Chemistry, Shahr-e-Qods Branch, Islamic Azad University, Tehran, Iran

such as plants, bacteria, fungi, yeast, and viruses act as, clean and eco-friendly precursors to prepare small size and stable nanoparticles [2, 3]. Using different plant parts for the synthesis of metal nanoparticles is the simplest and most cost-effective approach [4]. Among the various metal nanoparticles, iron and iron oxide nanoparticles (IONPs) have shown high potential in many industrial and biomedical applications. There are eight known iron oxides, among which hematite (α-Fe_2O_3), maghemite (γ-Fe_2O_3) and magnetite (Fe_3O_4) are very favorite and promising candidates [5]. Each of these three iron oxides has unique magnetic, catalytic, biochemical, and other properties, which are suitable for special biomedical and technical applications [6]. Hematite, as the most stable iron oxide with strongly antiferromagnetic properties, is widely used in gas sensors, pigments, catalysts, and as an oxidizer in thermite composition because of, its low cost and high resistor to corrosion [7]. It is also a precursor for the synthesis of maghemite (γ-Fe_2O_3) and magnetite (Fe_3O_4), which have been eagerly kept insight for both technological applications and scientific interests in recent years [8]. In particular, hematite can absorb visible light and so is considered as a cheap semiconductor and photo-catalyst [9–11].

Although chemical and physical methods are common for the synthesis of iron and iron oxide nanoparticles, various green and affordable synthesis protocols have been expanded employing plants and other biological systems. Desalegn et al. synthesized iron nanoparticles utilizing Mango peel extract without using any surfactant at room temperature [12]. They reported that the polyphenols in plant extract act as reducing and capping agents. Rostamizadeh et al. [13] synthesized Fe_2O_3 nanoparticles using fruit extract of Cornelian cherry in a simple and economic procedure. Markova et al. [14] reported the synthesis of iron (II, III)-polyphenol complex nanoparticles by green tea extract. Similar findings were reported by Nadagouda et al. [15] who evaluated that the size and morphology of iron nanoparticles are dependent on the extract concentration. Ahmmad et al. [16] synthesized highly pure α-Fe_2O_3 nanoparticles by using green tea (*Camellia sinensis*) leaf extract through a hydrothermal method. They synthesized spherical and highly porous nanoparticles with an average size of 60 nm. The leaf extract of Garlic Vine and $FeSO_4{\cdot}7H_2O$ were used for the synthesis of iron (III) oxide nanoparticles (β-Fe_2O_3), with a size of 18.22 nm by Prasad et al. [17]. They reported that the synthesized β-Fe_2O_3 undergoes a complete phase transformation to α-Fe_2O_3 at 500° C. Phumying et al. synthesized Fe_3O_4 nanoparticles by using Aloe Vera extract and ferric acetyl acetonate [$Fe(C_5H_8O_2)_3$]. The authors reported that by increasing the reaction time and temperature, the crystallinity of nanoparticles improve [18]. In another study, eucalyptus leaf extract was used for the synthesis of polydispersed iron nanoparticles [19]. FeO/Fe_3O_4 nanoparticles were synthesized by pomegranate leaf extract and the capacity of the bio nanocomposite for removing the pollutant hexavalent chromium from groundwater was evaluated [20]. Venkateswarlu et al. utilized plantain peel extract as a cost-effective bio-reducing agent to synthesize magnetite nanoparticles. They also evaluated the capacity of synthesized nanoparticles for removing dye and toxic metals from wastewater [21]. Senthil and Ramesh synthesized Fe_3O_4 nanoparticles by using *Tridax procumbens* leave extract. They reported that the plant extract includes the carbohydrates, which are responsible for nanoparticle synthesis [22].

Herein, we synthesized iron oxide nanoparticles (α-Fe_2O_3) by using ferric chloride solution and the aqueous extract of *Laurus nobilis* L. leave in a rapid and single-step method. The antibacterial and antifungal capacity of the synthesized nanoparticles were also evaluated in this research. *Laurus nobilis* L., which is commonly known as Bay (Family Lauraceae), is an ornamental plant native in the Mediterranean region. The plant is used as a traditional spice and have been mentioned for biological activities [23–28]. The structure and properties of the synthesized nanoparticles were evaluated by FT-IR and UV–Vis spectroscopy; XRD technique, SEM and TEM electron microscopy, and EDS technique. This study is in continuation of our previous effort for the synthesis of IONPs by aqueous extract of *L. nobilis* [29]. Herein, we optimized the biosynthesis procedure for IONPs and found better results, for example, the size of synthesized nanoparticles in this study were less than our previous report. Besides, the effect of the synthesized nanoparticles on some of the bacteria and fungi used in this project is being reported for the first time.

Material and methods

The used solvents and chemicals in this study were purchased from the Merck Company (Germany). XRD (EQUINOX 3000, Intel, France); FT-IR (Spectrum 100, Perkin Elmer, Germany); UV–Visible (UV.1800, Shimadzu, Japan); SEM (ZIGMAVP-500, Zeiss, Germany; EDS, Oxford Instruments, UK); Heater-Stirrer (MR Hei-End, Germany); Ultrasonic (S15H, Germany); Centrifuge (EBA 20 Hettich, Germany); Rotary evaporator (4003 Heidolph, Germany); Oven (Memmert 100–800, Germany).

The leaves of *Laurus nobilis* L. (Family Lauraceae) were collected from the north of Iran (province of Gilan) in June 2018. After washing and air-drying, the leaves were crushed into small pieces. Twenty gr of the leaves were soaked in 200 mL distilled water and was heated at 70 °C in 10 min. by a heater-stirrer (500 r/min). Finally, all the plant residues were removed by filtration and centrifugation of the extract.

The synthesis of Iron oxide nanoparticles was done by a green method. In brief, the as-prepared aqueous extract of

L. nobilis leaves (30 mL) and 0.1 M $FeCl_3{\cdot}6H_2O$ (30 mL) were mixed and stirred by a stirrer at room temperature. After 2.5 h, a dark precipitate appeared. For purification, the precipitate was repeatedly dispersed in ethanol and centrifuged. The dark brown-color solid product was dried in an oven at 250 °C for 12 h. Some factors like the volume and concentration of the precursors were optimized in the synthesis of IONPs. We used different techniques to characterize the synthesized nanoparticles. For the UV–Visible analysis, the product suspension (1 mL) was sonicated for 15 min (4000 rpm) and was monitored at 200–800 nm. The synthesized nanoparticles were analyzed by FT-IR technique using the KBr pellet method. UV–Visible and FT-IR analysis were also recorded for the plant extract at the same conditions as the nanoparticles. The X-ray diffraction analysis was used for identifying the phase structure of the synthesized particles. To visualize the size and morphology of the particles, SEM and TEM techniques were utilized. EDS analysis was applied for identifying the elemental composition of the nanoparticles.

The antimicrobial activity of the synthesized IONPs was evaluated against three pathogenic bacteria, *Staphylococcus aureus* (PTCC 1189), *Escherichia coli* (ATCC 23922), *Listeria monocytogenes* (PTCC 1294) and also against two fungi, *Aspergillus flavus* (PTCC 5004) and *Penicillium spinulosum* (PTCC 5251) by using the disk diffusion method [30]. Mueller Hinton agar (Merck), which had been adjusted to 0.5 McFarland standard, was used to culture the bacteria using a sterile swab. Moreover, the culture medium of sabouraud dextrose agar (Merck) containing Chloramphenicol antibiotic was used to culture the fungi. Wells of 6.4 mm diameter was punched over the agar plates and then, 4 mg of nanoparticle powder was poured into the wells. The standard antibiotics: Tetracycline (30 mcg/disc), Kanamycine (5 mcg/disc), Sulfamethoxazole (5 mcg/disc), Amoxicillin (25 mcg/disc), Cefixime (5 mcg/disc), Oxacilline (1 mcg/disc), Penicillin (10 unit/disc), Novobiocin (30 mcg/disc) and Nystatin (100 mcg/disc) which were purchased from the companies Padtan Teb (Iran) and Himedia (India), were used as positive controls. Finally, the plates were incubated at 37 °C for 24 h for the bacteria and 72 h (37 °C) for the fungi. After the incubation, the zone of inhibition around each well was measured.

Results and discussion

In this study, we applied a biosynthetic method for producing IONPs by the aqueous extract of *L. nobilis* leaves. As shown in Fig. 1, the pale brown color of the extract solution was changed to dark brown, during the synthesis of IONPs. This discoloration is a sign of iron oxide formation, which has been reported many times in other papers [17–22].

The UV–Visible absorption spectra of the aqueous extract of *L. nobilis* leaves were observed in both the absence and presence of IONPs at 200–800 nm. The maximum absorbance at 285 nm indicated the formation of IONPs (Fig. 2). This is quite similar to those previously were reported for α-Fe_2O_3 nanoparticles [31, 32].

To identify the biomolecules, which may be responsible for the reduction process, we used infrared spectroscopy (Fig. 3). The peaks at (600, 450) cm^{-1} correspond to Fe–O stretching vibration in the phase hematite, which is reported previously in the literature [33]. The signals at (3700–3400) cm^{-1} are due to O–H stretching for the OH group with a hydrogen bond. This functional group is abundant in natural compounds such as alcohols, flavonoids, and polyphenols. Since some iron hydroxide molecules may be formed during the synthesis procedure (the XRD results confirms), the observed signal can also be owing to the corresponding OH group. The peaks around (1623–1416) cm^{-1} correspond to C=C stretching in aromatic compounds and the peak observed at 1100 cm^{-1} is due to C–C stretching vibrations. The results of FT-IR spectra for the L. nobilis aqueous extract and the synthesized IONPs shows the presence of biomolecules around the nanoparticles as capping agents and confirms that the natural compounds in the extract have taken a role in the synthesis and stability of IONPs.

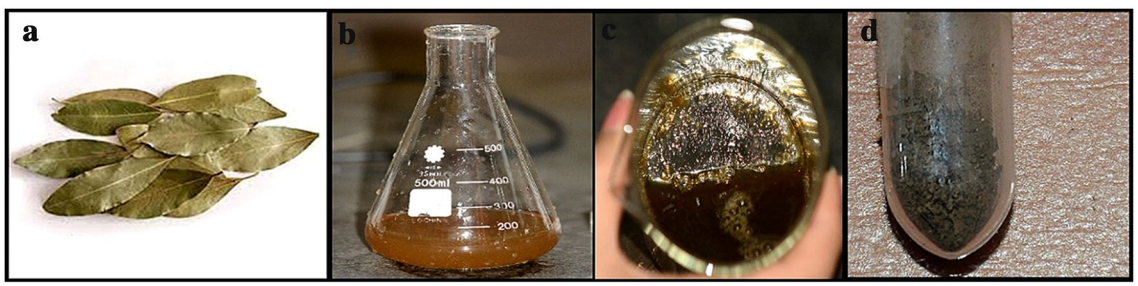

Fig. 1 Photograph of the aqueous extract of *Laurus nobilis* leaves (**a**), aqueous extract of *L. nobilis* (**b**), color change of the extract (**c**), and α-Fe_2O_3 nanoparticles (**d**)

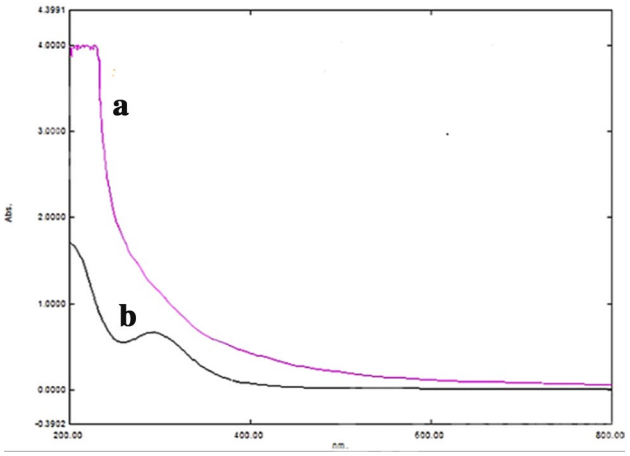

Fig. 2 UV–Visible spectra of the aqueous extract of *Laurus nobilis* leaves (**a**), and synthesized α-Fe_2O_3 nanoparticles/*L. nobilis* extract mixture (**b**)

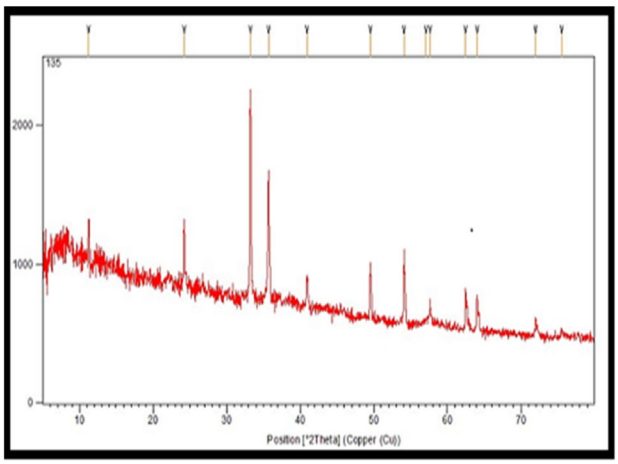

Fig. 4 XRD pattern of α-Fe_2O_3 nanoparticles synthesized by the aqueous extract of *Laurus nobilis* leaves

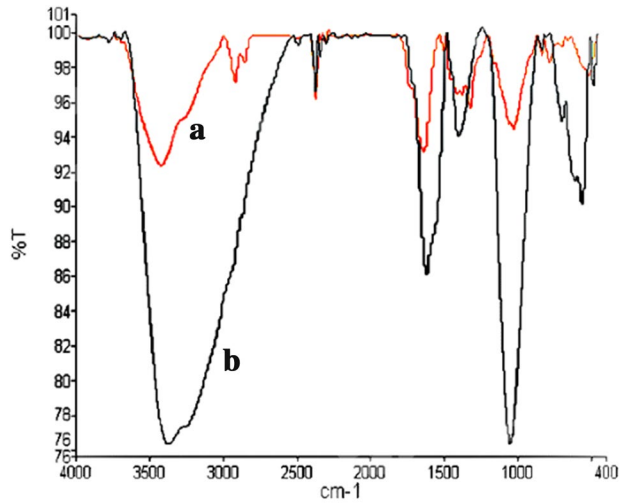

Fig. 3 FT-IR spectrum of the aqueous extract of *Laurus nobilis* leaves (**a**), and synthesized α-Fe_2O_3 nanoparticles (**b**)

The crystalline structure and phase identification of the nanoparticles were characterized by X-ray powder diffraction analysis. The intensive and sharp peaks in the XRD analysis (Fig. 4) revealed that the synthesized nanoparticles are highly crystalline and perfectly consistent with the standard values for the hexagonal rhombohedral α-Fe_2O_3 phase (JCPDS-33-0664). Furthermore, the synthesized nanoparticles can be considered as photocatalyst because of the strong sharp peaks at 2θ values around 33.2 and 35.6, which are indexed to the preferential orientations along (104) and (110) planes respectively [34]. The crystalline size of the synthesized nanoparticles was estimated at 21.5 nm from the most intense peak at $2\theta = 33.2°$ using Scherer's equation ($D = K\omega/\beta\cos\theta$). In this equation, K is the shape factor for a typical value of 0.9; β (2θ) is the full width at half-maximum (FWHM) of a particular diffraction peak in radians; ω is the X-ray wavelength (for copper, $\omega = 1.5406$ Å), and θ is the Bragg angle. The XRD result in this study is consistent with the recent reports on iron oxides [34–38]. A list of Bragg reflections and corresponding lattice planes (*hkl*) are presented in Table 1. The diffraction pattern in our study is well-matched with the others, especially with the results presented by Peng et al. and Ocwieja et al. [35, 36]. The most intensive peak in our study was seen at $2\theta = 33.2°$ in accordance with three of the mentioned reports in Table 1. While two others reported the peaks at 2θ values around 35.5° and 36.2°, as the most intense peak. The diffraction peak with low intensity observed at $2\theta = 11.2°$ in the XRD pattern of our study, which is not seen in the other samples, maybe due to the formation of iron hydroxide nanoparticles which have not been transformed to α-Fe_2O_3 Phase [39, 40]. The size of nanoparticles in the mentioned studies, reported about (20, 40, 22, and 40) nm respectively, except for the result presented by Peng et al., which shows that the synthesized particles are two-dimensional microplates of 2–10 µm. The result of our study looks good in comparison with the other samples in Table 1.

The FESEM image and EDS spectra for the IONPs are shown in (Fig. 5a, b) respectively. From the FESEM image, we can see that the nanoparticles are spherical like and in the range of nano. The elemental composition

Table 1 The Bragg reflections peaks and the assigned lattice planes (*hkl*) in this study in comparison with some other reports

Peak position 2θ (°)						
A	B	C	D	E	F	*hkl*
11.2	-	–	–	–	–	1 1 0
24.2	24.3	23.9	24.1	23.9	23.9	0 1 2
33.2	**33.2**	33.0	**33.2**	**33.2**	33.5	1 0 4
35.7	35.9	**35.5**	35.6	35.5	**36.3**	1 1 0
–	–	–	39.7	39.8	–	0 0 6
40.9	41.2	40.5	40.9	–	41.5	1 1 3
49.5	49.4	49.3	49.6	49.6	49.6	0 2 4
54.1	54.1	53.9	53.9	53.9	54.3	1 1 6
57.6	57.6	–	57.6	57.5	57.8	0 1 8
62.5	62.5	62.1	62.5	62.8	63.4	2 1 4
64.0	64.1	63.8	64.1	64.1	64.7	3 0 0
–	–	–	69.8	–	–	2 0 8
71.9	–	–	72.1	72.3	–	0 1 0
75.5	–	–	75.9	75.6	–	2 2 0

A our results, *B* Ref. [33], *C* Ref. [34], *D* Ref. [35], *E* Ref. [36], *F* Ref. [37]

The most intense peak in each case is bolded

analysis of the IONPs revealed the presence of Fe and O in the sample and confirmed high purity for the synthesized IONPs. The relative percentage of iron and oxygen in the synthesized nanoparticles (69.23% and 22.36% respectively) are similar to the theoretical expected stoichiometric mass percent.

The TEM photograph of the synthesized IONPs is depicted in Fig. 6. The average particle size was found 8.03 ± 8.99 nm for 206 individual selections. As it is seen, the nanoparticles are almost spherical like and partly as a hexagonal shape. The average size of synthesized nanoparticles shows some difference with the size of particles found by Scherer's equation in the XRD spectra. It may be due to the wide range size distribution of the nanoparticles, given the SD value calculated from the TEM analysis.

Antimicrobial activity of the synthesized nanoparticles revealed moderate activity against the Gram-positive bacterium of *Listeria monocytogenes* (12 mm) and also against two fungi, *Aspergillus flavus* (13 mm) and *Penicillium spinulosum* (14 mm) (Fig. 7; Table 2). It has been reported that calcination may decompose the surface-attached phytochemicals as capping agents and diminishes the advanced biomedical applications of nanoparticles [41]. Therefore, we used nanoparticles before the calcination process to evaluate the antimicrobial activity. The mechanism by which the IONPs shows antibacterial activity may be due to the oxidative stress process caused by reactive oxygen species (ROS), which can damage biological macromolecules [42–44]. There are some reports on the antimicrobial activity of hematite nanoparticles in the literature. Mohamad Rafi et al. evaluated the antibacterial activity of hematite nanoparticles on some pathogenic bacteria. According to their report, the best results were found for the Gram (+) bacteria *Aeromunas hydrophila* and the Gram (−) bacteria *Escherichia coli* [45]. Rufus et al. synthesized α-Fe_2O_3 nanostructures using the extract of guava (*Psidium guajava*) leaves. They reported hematite nanoparticles as potent antibacterial compounds against Gram-positive and Gram-negative bacteria [46]. In another study, the antibacterial potential of green synthesized hematite nanoparticles was investigated against nine pathogenic bacterial strains using the disc diffusion method. The bacterial strains including *Salmonella typhi, Staphylococcus aureus*, *Salmonella enterica,* and *Klebsiella pneumonia* were found as the most susceptible to the IONPs [47]. Another study of bactericidal effects and concentration dependence of IONPs on *Staphylococcus epidermidis* was reported by Taylor and Webster [48]. Anti-fungal activities of hematite nanoparticles have also been studied previously. The highest zone of inhibition was reported against *Penicillium chrysogenum* (28.67 mm) followed by *Aspergillus niger* (26.33 mm), *Trichothecium roseum* (22.67 mm), *Alternaria alternata* (21.33 mm) [49]. To the best of our knowledge, the antimicrobial activity of hematite nanoparticles against the bacterium *L. monocytogenes* and the fungus *A. flavus* and *P. spinulisum,* is reporting here for the first time.

It is not found that how living organisms can help the bioreduction process and synthesis of nanoparticles. However,

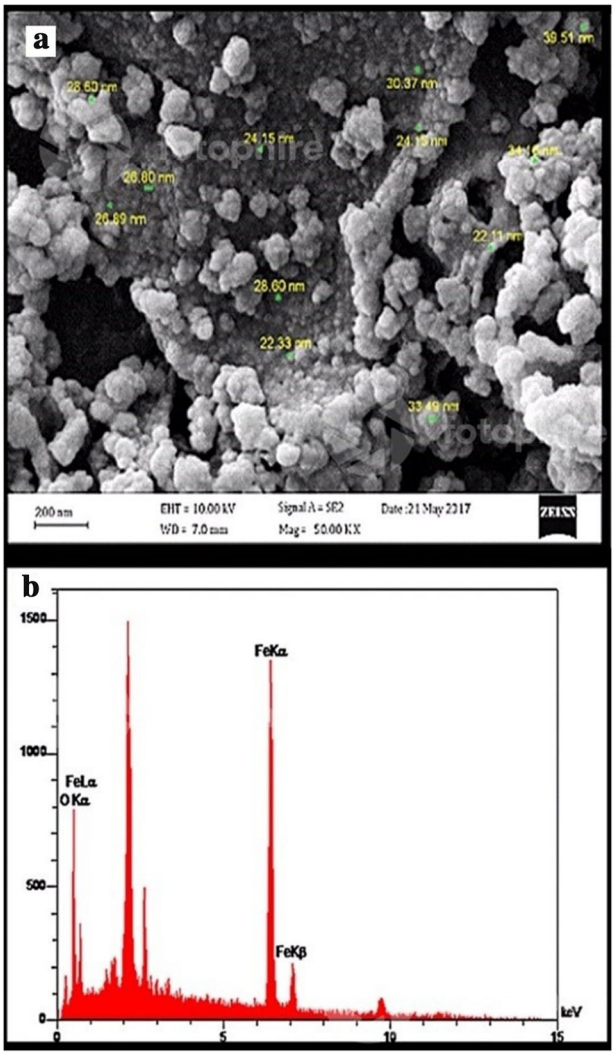

Fig. 5 FESEM image (**a**), and EDS spectra of α-Fe_2O_3 nanoparticles synthesized by the aqueous extract of *Laurus nobilis* leaves (**b**)

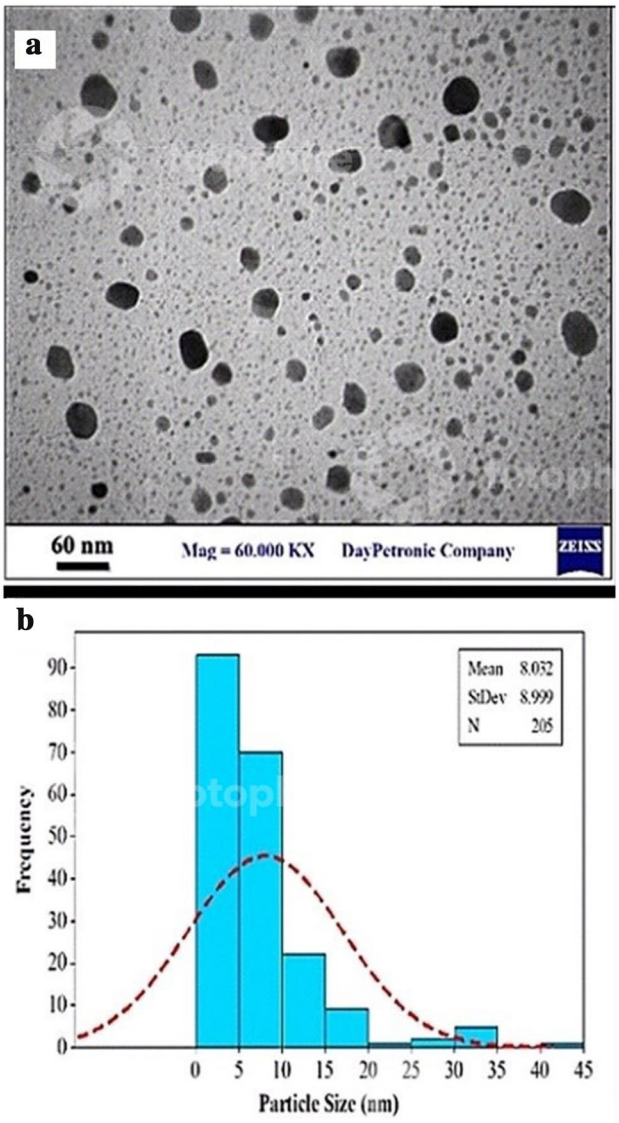

Fig. 6 TEM image (**a**), size distribution and Gaussian fitting of monodispersed α-Fe_2O_3 nanoparticles (**b**) synthesized by the aqueous extract of *Laurus nobilis* leaves

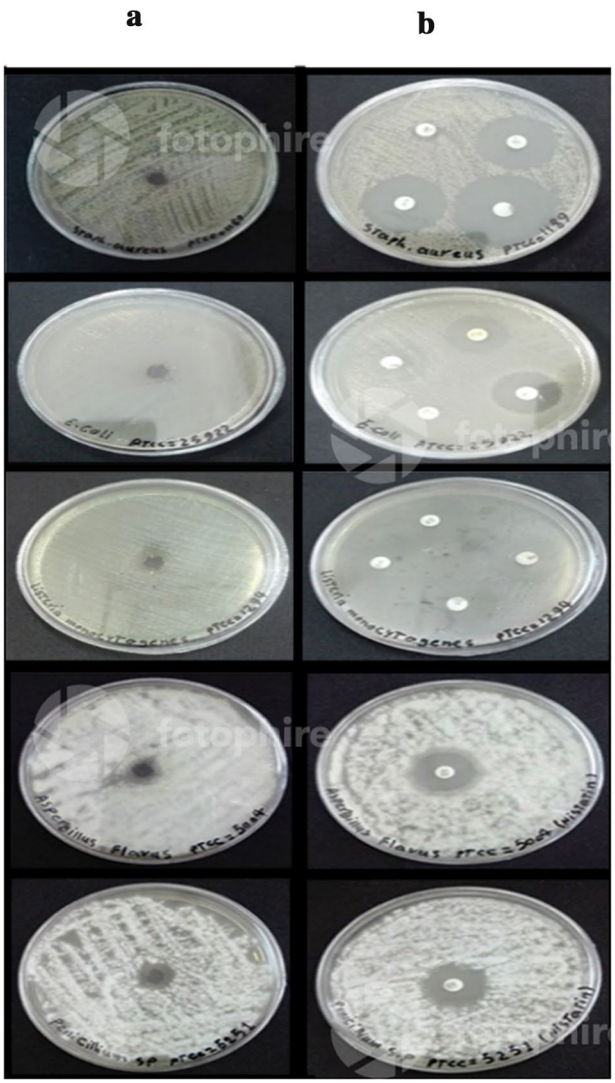

Fig. 7 Anti-microbial activity of (**a**) α-Fe_2O_3 nanoparticles synthesized by the aqueous extract of *Laurus nobilis* leaves, and (**b**) the reference antibiotics

it is proposed that the biomolecules in plant extracts and the enzymes, which are produced by bacteria or fungi, may be responsible for the reduction of the ionized salts and establishment of the respective nanoparticles [50–53]. Generally, the nanoparticles synthesized by using the natural compounds present in the living organisms, are biocompatible. Previous studies have shown the role of *L. nobilis* leaves extracts in the synthesis of silver and gold nanoparticles [54–56]. Antimicrobial and antioxidant activities of the plant extract have also been reported previously [57].

A critical need in the field of nanotechnology is the development of eco-friendly and reliable processes for the synthesis of metal oxide nanoparticles. In this project, we demonstrated the synthesis of α-Fe_2O_3 nanostructures by using the aqueous extract of *L. nobilis* leaves and 0.1 M $FeCl_3{\cdot}6H_2O$ as precursors. The synthesized nanoparticles were crystalline and spherical like and partly as a hexagonal shape with an average size of 8.09 ± 8.99 nm. This medicinal plant includes the natural compounds, which are responsible for the bioreduction process. Antimicrobial activity of the synthesized nanoparticles was also evaluated in this study. Our results confirm that the proposed route, using $FeCl_3$ and the aqueous extract of *L. nobilis* as precursors, is a simple, low cost, non-toxic and ecofriendly approach for the production of α-Fe_2O_3 nanoparticles, which can be considered as a potent antimicrobial compound. Currently, controlling the size and shape of nanoparticles, and finding the exact mechanism of IONPs preparation by living organisms, need much more attention and experimentation.

Table 2 Antimicrobial activity of the synthesized Iron oxide nanoparticles by *Laurus nobilis* L. leaves aqueous extract

		Inhibition zone diameter (mm)									
Gram (±) bacteria and/or fungi	PTCC/ATCC	IONPs	A	C	S	T	K	O	P	No	Ni
Staphylococcus aureus (+)	1189[a]	0	NT[c]	0	31	NT	26	24	NT	NT	NT
Escherichia coli (−)	23922[b]	0	NT	21	26	20	NT	NT	NT	NT	NT
Listeria monocytogenes (+)	1294[a]	12	22	NT	NT	31	NT	NT	10	27	NT
Aspergillus flavus	5004[a]	13	NT	NT	NT	NT	NT	NT	NT	NT	20
Penicillium spinulosum	5251[a]	14	NT	NT	NT	NT	NT	NT	NT	NT	19

a Persian type culture, *b* (ATCC) American type culture, *C* not tested, *A* amoxicillin, *C* cefixime, *S* sulfamethoxazole, *T* tetracycline, *K* kanamycin, *O* oxacilline, *A* amoxicillin, *P* penicillin, *No* novobiocin, *Ni* nistatin

References

1. Michna, A., Morga, M., Adamczyk, Z., Kubiak, K.: Monolayers of silver nanoparticles obtained by green synthesis on macroion modified substrates. Mater. Chem. Phys. **227**, 224–235 (2019)
2. Fang, X., Wang, Y., Wang, Z., Jiang, Z., Dong, M.: Microorganism assisted synthesized nanoparticles for catalytic applications, review. Energies **12**, 190 (2019)
3. Kumar, V.G.V., Prem, A.A.: Green synthesis and characterization of iron oxide nanoparticles using *Phyllanthus niruri* extract. Orient. J. Chem. **34**, 2583–2589 (2018)
4. Iravani, S.: Green synthesis of metal nanoparticles using plants. Green Chem. **13**, 2638–2650 (2011)
5. Deraz, N.M., Abd-Elkader, O.H.: Investigation of magnesium ferrite spinel solid solution with iron-rich composition. Int. J. Electrochem. Sci. **8**, 9071–9081 (2013)
6. Zolghadr, S., Khojier, K., Kimiagar, S.: Ammonia sensing properties of α-Fe_2O_3 thin films during post annealing process. Procedia Mater. Sci. **11**, 469–473 (2015)
7. Campos, E.A., Pinto, D.V.B.S., Oliveira, J.I.S., Mattos, E.C., Dutra, R.C.L.: Synthesis, characterization and applications of iron oxide nanoparticles—a short review. J. Aerosp. Technol. Manag. **7**, 267–276 (2015)
8. Prasad, C., Tang, H., Liu, W.: Magnetic Fe_3O_4 based layered double hydroxides (LDHs) nanocomposites (Fe_3O_4/LDHs): recent review of progress in synthesis, properties and applications. J. Nanostructure Chem. **8**, 393–412 (2018)
9. Samrot, A.V., Rashmitha, S., Veera, P., Sahithya, C.S.: *Azadirachta indica* influenced biosynthesis of super-paramagnetic iron-oxide nanoparticles and their applications in tannery water treatment and X-ray imaging. J. Nanostructure Chem. **8**, 343–351 (2018)
10. Liu, Y., Yu, L., Hu, Y., Guo, C., Zhang, F., Lou, X.W.: A magnetically separable photocatalyst based on nest-like γ-Fe_2O_3/ZnO double-shelled hollow structures with enhanced photocatalytic activity. Nanoscale **4**, 183–187 (2012)
11. Lohrasbi, S., Jadidi Kouhbanani, M.A., Beheshtkhoo, N., Ghasemi, Y., Amani, A.M., Taghizadeh, S.: Green synthesis of iron nanoparticles using *Plantago major* leaf extract and their application as a catalyst for the decolonization of azo dye. BioNanoScienc **9**, 317–322 (2019)
12. Desalegn, B., Megharaj, M., Zuliang Chen, Z., Naidu, R.: Green synthesis of zero valent iron nanoparticle using mango peel extract and surface characterization using XPS and GC-MS. Heliyon **5**, 1–9 (2019)
13. Rostamizadeh, E., Iranbakhsh, A., Majd, A., Arbabian, S., Mehragan, I.: Green synthesis of Fe_2O_3 nanoparticles using fruit extract of *Cornus mas* L. and its growth-promoting roles in barley. J. Nanostruct. Chem. **2**, 422–427 (2020)
14. Markova, Z., Novak, P., Kaslik, J., Plachtova, P., Brazdova, M., Jancula, D., Siskova, K.M., Machala, L., Marsalek, B., Zboril, R.: Iron (II, III)-Polyphenol complex nanoparticles derived from green tea with remarkable eco toxicological impact. ACS Sustain. Chem. Engin. **2**, 1674–1680 (2014)
15. Nadagouda, M.N., Castle, A.B., Murdock, R.C., Hussain, S.M., Varma, R.S.: In vitro biocompatibility of nanoscale zero-valent iron particles (NZVI) synthesized using tea polyphenols. Green Chem. **12**, 114–122 (2010)
16. Ahmmad, B., Leonard, K., Shariful Islam, M., Kurawaki, J., Muruganandham, M., Ohkubo, T., Kuroda, Y.: Green synthesis of mesoporous hematite (α-Fe_2O_3) nanoparticles and their photocatalytic activity. Adv. Powder Technol. **24**, 160–167 (2013)
17. Prasad, A.S.: Iron oxide nanoparticles synthesized by controlled bio-precipitation using leaf extract of Garlic Vine (*Mansoa alliacea*). Mat. Sci. Semicon. Proc. **53**, 79–83 (2016)
18. Phumying, S., Labuayai, S., Thomas, C., Amornkitbamrung, V., Swatsitang, E., Maensiri, S.: Aloe Vera plant-extracted solution hydrothermal synthesis and magnetic properties of magnetite (Fe_3O_4) nanoparticles. Appl. Phys. A. **111**, 1187–1193 (2012)
19. Wang, Z., Fang, C., Megharaj, M.: Characterization of iron-polyphenol nanoparticles synthesized by three plant extracts and their fenton oxidation of azo dye. ACS Sustain. Chem. Eng. **2**, 1022–1025 (2014)
20. Rao, A., Bankar, A., Kumar, A.R., Gosavi, S., Zinjarde, S.: Removal of hexavalent chromium ions by *Yarrowia lipolytica* cells modified with phyto-inspired Fe^0/Fe_3O_4 nanoparticles. J. Contam. Hydrol. **146**, 63–73 (2013)
21. Venkateswarlu, S., Rao, Y.S., Balaji, T., Prathima, B., Jyothi, N.V.: Biogenic synthesis of Fe_3O_4 magnetic nanoparticles using plantain peel extract. Mat. Lett. **100**, 241–244 (2013)
22. Senthil, M., Ramesh, C.: Biogenic synthesis of Fe_3O_4 nanoparticles using *Tridax procumbens* leaf extract and its antibacterial activity on *Pseudomonas aeruginosa*. Dig. J. Nanomater. Bios. **7**, 1655–1660 (2012)
23. Ouchikh, O., Chahed, T., Ksouri, R., Taarit, M.B., Faleh, H., Abdelly, C., Kchouk, M.E., Marzouk, B.: The effects of extraction method on the measured tocopherol level and antioxidant activity of *L. nobilis* vegetative organs. J. Food Compos. Anal. **24**, 103–110 (2011)
24. Fidan, H., Stefanova, G., Kostova, I., Stankov, S., Damyanova, S., Stoyanova, A., Zheljazkov, V.D.: Chemical composition and antimicrobial activity of *Laurus nobilis* L. essential oils from Bulgaria. Molecules **24**, 804 (2019)
25. Conforti, F., Statti, G., Uzunov, D., Menichinia, F.: Comparative chemical composition and antioxidant activities of wild and cultivated *Laurus nobilis* L. leaves and Foeniculum vulgare subsp. piperitum (Ucria) coutinho seeds. Biol. Pharm. Bull. **29**, 2056–2064 (2006)
26. Fernandez-Andrade, C., Da Rosa, M., Boufleuer, E., Ferreira, F., Iwanaga, C., Gonçalves, J., Cortez, D., Martins, C., Linde, G., Simões, M.: Chemical composition and antifungal activity of essential oil and fractions extracted from the leaves of *Laurus nobilis* L. cultivated in southern Brazil. J. Med. Plants Res. **48**, 865–871 (2016)
27. Speroni, E., Cervellati, R., Dall'Acqua, S., Guerra, M.C., Greco, E., Govoni, P., Innocenti, G.: Gastro protective effect and antioxidant properties of different *Laurus nobilis* L. leaf extracts. J. Med. Food **14**, 499–504 (2011)
28. Caputo, L., Nazzaro, F., Souza, L.F., Aliberti, L., De Martino, L., Fratianni, F., Coppola, R., De Feo, V.: *Laurus nobilis*: composition of essential oil and its biological activities. Molecules **22**, 930–941 (2017)
29. Kamari M., Jamzad, M., Naderi, F.: Green synthesis of iron oxide nanoparticles by *Laurus nobilis* L. aqueous extract. Poster session presented at: The 25th Iranian Seminar of Organic Chemistry, Tehran, 2–4 Sept 2017.
30. Bauer, A.W., Kirby, W.M.M., Sherris, J.C., Truch, M.: Antibiotic susceptibility testing by standardized single disk method. Am. J. Clin. Pathol. **45**, 493–496 (1996)
31. Klacanova, K., Fodran, P., Simon, P., Rapta, P., Boca, R., Jorik, V., Miglierini, M., Kolek, E., Kaplovik, L.: Formation of Fe (0)-Nanoparticles via reduction of Fe (II) compounds by amino acids and their subsequent oxidation to Iron Oxides. J. Chem. **2013**, 1–10 (2013)
32. Kanagasubbulakshmi, S., Kadirvelu, K.: Green synthesis of Iron oxide nanoparticles using *Lagenaria siceraria* and evaluation of its antimicrobial activity. Def. Life Sci. J. **2**, 422–427 (2017)
33. Rajendran, K., Karunagaran, V., Mahanty, B., Sen, S.: Biosynthesis of hematite nanoparticles and its cytotoxic effect on HepG2 cancer cells. Int. J. Biol. Macromol. **74**, 376–381 (2015)

34. Ilmetov, R.: Photocatalytic activity of hematite nanoparticles prepared by sol-gel method. Mater. Today: Proc. **6**, 11–14 (2019)
35. Joshi, D.P., Pant, G., Arora, N., Nainwal, S.: Effect of solvents on morphology, magnetic and dielectric properties of (α-Fe_2O_3@SiO_2) core-shell nanoparticles. Heliyon **3**, 1–16 (2017)
36. Abusalem, M., Awwad, A., Ayad, J., Abu Rayyan, A.: Green synthesis of α-Fe_2O_3 nanoparticles using pistachio leaf extract influenced seed germination and seedling growth of tomatoes. JJEES **10**, 161–166 (2019)
37. Peng, D., Beysen, S., Li, Q., Yang, L.: Hydrothermal synthesis of monodisperse α-Fe_2O_3 hexagonal platelets. Particuology **8**, 386–389 (2010)
38. Ocwieja, M., Adamczyk, Z., Morga, M., Bielanska, E., Wegrzynowicz, A.: Hematite nanoparticle monolayers on mica preparation by controlled self-assembly. J. Colloid Interf. Sci. **386**, 51–59 (2012)
39. Asoufi, H.M., Al-Antary, T.M., Awwad, A.M.: Green route for synthesis hematite (α-Fe_2O_3) nanoparticles: Toxicity effect on the green peach aphid, *Myzus persicae* (Sulzer). Environ. Nanotechnol. Monit. Manag. **9**, 107–111 (2018)
40. Xu, C., Cheng, D., Gao, B., Yin, Z., Yue, Q.: Zhao X (2012) Preparation and characterization of β-FeOOH-coated sand and its adsorption of Cr(VI) from aqueous solutions. Front. Environ. Sci. Eng. **6**, 455–462 (2012)
41. Singh, B.P., Sharma, N., Kumar, R., Kumar, A.: Simple hydrolysis synthesis of uniform rice-shaped β-FeOOH nanocrystals and their transformation to α-Fe_2O_3 microspheres. Indian J. Mater. Sci. **2015**, 1–7 (2015)
42. Marslin, G., Siram, K., Maqbool, Q., Selvakesavan, R.K., Kruszka, D., Kachlicki, P., Franklin, G.: Secondary metabolites in the green synthesis of metallic nanoparticles. Materials **11**, 940 (2018)
43. Turakhia, B., Chikkala, S., Shah, S.: Novelty of bioengineered iron nanoparticles in nano coated surgical cotton: a green chemistry. Adv. Pharmacol. Sci. **2019**, 1–10 (2019)
44. Tran, N., Mir, A., Mallik, D., Sinha, A., Nayar, S., Webster, T.J.: Bactericidal effect of iron oxide nanoparticles on *Staphylococcus aureus*. Int. J. Nanomed. **5**, 277–283 (2010)
45. Subbulakshmi, K., Kadirvelu, K.: Green synthesis of iron oxide nanoparticles using *Lagenaria siceraria* and evaluation of its antimicrobial activity. Def.Life Sci. J. **2**, 422–427 (2017)
46. Mohamad Rafi, M., Zameer Ahmed, K.S., Prem Nazar, K., Siva Kumar, D., Thamilselvan, M.: Synthesis, characterization and magnetic properties of hematite (α-Fe_2O_3) nanoparticles on polysaccharide templates and their antibacterial activity. Appl. Nanosci. **5**, 515–520 (2015)
47. Rufus, A., Sreeju, N., Philip, D.: Synthesis of biogenic hematite (α-Fe_2O_3) nanoparticles for antibacterial and nanofluid applications. RSC Adv. **6**, 94206–94217 (2016)
48. Hassan, D., Talha Khalil, A., Saleem, J., Diallo, A., Khamlich, S., Shinwari, Z.K., Malik Maaza, M.: Biosynthesis of pure hematite phase magnetic iron oxide nanoparticles using floral extracts of *Callistemon viminalis* (bottlebrush): their physical properties and novel biological applications. Artif. Cell Nanomed. B. **46**, 693–707 (2018)
49. Taylor, E.N., Webster, T.J.: The use of superparamagnetic nanoparticles for prosthetic biofilm prevention. Int. J. Nanomed. **4**, 145–152 (2009)
50. Parveena, S., Wania, A.H., Shahb, M.A., Devib, H.S., Bhata, M.Y., Koka, J.A.: Preparation, characterization and antifungal activity of iron oxide nanoparticles. Microb. Pathog. **115**, 287–292 (2018)
51. Bharde, A.A., Parikh, R.Y., Baidakova, M., Jouen, S., Hannoyer, B., Enoki, T., Prasad, B., Shouche, Y.S., Ogale, S., Sastry, M.: Bacteria-mediated precursor-dependent biosynthesis of superparamagnetic iron oxide and iron sulfide nanoparticles. Langmuir **24**, 5787–5794 (2008)
52. Salgado, P., Márquez, K., Rubilar, O., Contreras, D., Vidal, G.: The effect of phenolic compounds on the green synthesis of iron nanoparticles (Fe_xO_y-NPs) with photocatalytic activity. Appl. Nanosci. **9**, 371–385 (2019)
53. Luo, F., Chen, Z., Megharaj, M., Naidu, R.: Biomolecules in grape leaf extract involved in one-step synthesis of iron-based nanoparticles. RSC Adv. **4**, 53467–53474 (2014)
54. Khalil, M.M.H., Mahmoud, I.I., Hamed, M.O.A.: Green synthesis of gold nanoparticles using *Laurus nobilis* L. leaf extract and its antimicrobial activity. IJGHC **4**, 265–279 (2015)
55. Kashkouli, S., Jamzad, M., Nouri, A.: Total phenolic and flavonoids contents, radical scavenging activity and green synthesis of silver nanoparticles by *Laurus nobilis* L. leaves aqueous extract. JMPB **1**, 25–32 (2018)
56. Al-Ghamdi, A.Y.: Antimicrobial and catalytic activities of green synthesized silver nanoparticles using bay laurel (*Laurus nobilis*) leaves extract. J. Biomater. Nanobiotech. **10**, 26–39 (2019)
57. Muniz-Marquez, D.B., Rodriguez, R., Balagurusamy, N., Carrillo, M.L., Belmares, R., Contreras, J.C., Nevarez, G.V., Aguilar, C.N.: Phenolic content and antioxidant capacity of extracts of *Laurus nobilis* L., *Coriandrum sativum* L. and *Amaranthus hybridus* L. CYTA J. Food **12**, 271–276 (2014)